

# Plasma-Based Advanced Accelerators at the Brookhaven Accelerator Test Facility

I. V. Pogorelsky<sup>1</sup>, M. Babzien<sup>1</sup>, K. P. Kusche<sup>1</sup>, I. V. Pavlishin<sup>1</sup>, V. Yakimenko<sup>1</sup>,  
C. E. Dilley<sup>2</sup>, S. C. Gottschalk<sup>2</sup>, W. D. Kimura<sup>2</sup>, T. Katsouleas<sup>3</sup>, P. Muggli<sup>3</sup>, E. Kallos<sup>3</sup>,  
L. C. Steinhauer<sup>4</sup>, A. Zigler<sup>5</sup>, N. Andreev<sup>6</sup>, D. B. Cline<sup>7</sup>, and F. Zhou<sup>7</sup>

<sup>1</sup> Brookhaven National Laboratory, Accelerator Test Facility, Upton, NY, USA

<sup>2</sup> STI Optronics, Inc., Bellevue, WA, USA

<sup>3</sup> University of Southern California, Los Angeles, CA, USA

<sup>4</sup> University of Washington, Redmond Plasma Physics Laboratory, Redmond, WA, USA

<sup>5</sup> Hebrew University, Jerusalem, Israel

<sup>6</sup> Institute of High Density Energy, Moscow, Russia

<sup>7</sup> University of California at Los Angeles, Los Angeles, CA, USA

e-mail: igor@bnl.gov

Received August 31, 2005

**Abstract**—The Accelerator Test Facility at Brookhaven National Laboratory (BNL ATF) offers to its users a unique combination of research tools that include a high-brightness 70-MeV electron beam, a mid-infrared ( $\lambda = 10 \mu\text{m}$ ) CO<sub>2</sub> laser of terawatt power, and a capillary discharge as a plasma source. These cutting-edge technologies have enabled us to launch a new R&D program at the forefronts of advanced accelerators and radiation sources. The main subjects that we are researching are innovative methods of producing wakes in a linear regime using plasma resonance with the electron microbunch train periodic to the laser’s wavelength and so-called “seeded” laser wakefield acceleration (LWFA) that is driven and probed by a combination of electron and laser beams. We describe the present status of the ATF experimental program, including simulations and preliminary experiments; in addition, we review previous ATF experiments that were the precursors to the present program. They encompass our demonstration of longitudinal- and transverse-field phasing inside the plasma wave, plasma channeling of intense CO<sub>2</sub> laser beams, and the generation of *e*-beam microbunch trains by the inverse FEL technique.

DOI: 10.1134/S1054660X06020095

## INTRODUCTION

The BNL ATF provides a setting to search for new methods of electron acceleration. For this purpose, the ATF is equipped with a high-brightness electron linac and high-power lasers that include a Nd : YAG laser used primarily to drive a photocathode gun for injecting picosecond electron bunches into a linac and a CO<sub>2</sub> laser used for laser-beam interaction tests that are set in linac beamlines in a fully equipped experimental hall.

Several world-class experiments and breakthrough results obtained at the ATF over the last decade put this facility among the leading ones in research on advanced accelerators and radiation sources. BNL ATF has demonstrated inverse Cherenkov and inverse FEL electron acceleration, including the first staged laser acceleration experiment STELLA, has advanced visible FEL research, explored the first High Gain Harmonic Generation FEL, and attained the highest yield in Thomson X-ray scattering. Other recent research has focused on demonstrating nonlinear Thomson scattering, along with pioneering work in RF injectors and accelerator diagnostics.

A newly acquired plasma-channel technology further broadens the ATF capabilities, thereby allowing the research program to expand into plasma-based methods of electron acceleration. The recent integration of the plasma source into the electron beamline, together with the demonstration of laser channeling and plasma wakefield generation with electron beams, built a foundation for next-generation plasma-based electron acceleration experiments that include seeded self-modulated LWFA and resonant multibunch plasma wakefield acceleration (PWFA).

## TERAWATT PICOSECOND CO<sub>2</sub> LASER

The terawatt picosecond CO<sub>2</sub> laser is perhaps the most unique component of the ATF and deserves special attention here. CO<sub>2</sub> lasers have at least two invaluable features, both based on their wavelength, which is ten times longer than that of solid state lasers. The first advantage is that the CO<sub>2</sub> laser wavelength offers a viable compromise between conventional low-emittance RF accelerators and high-gradient optical

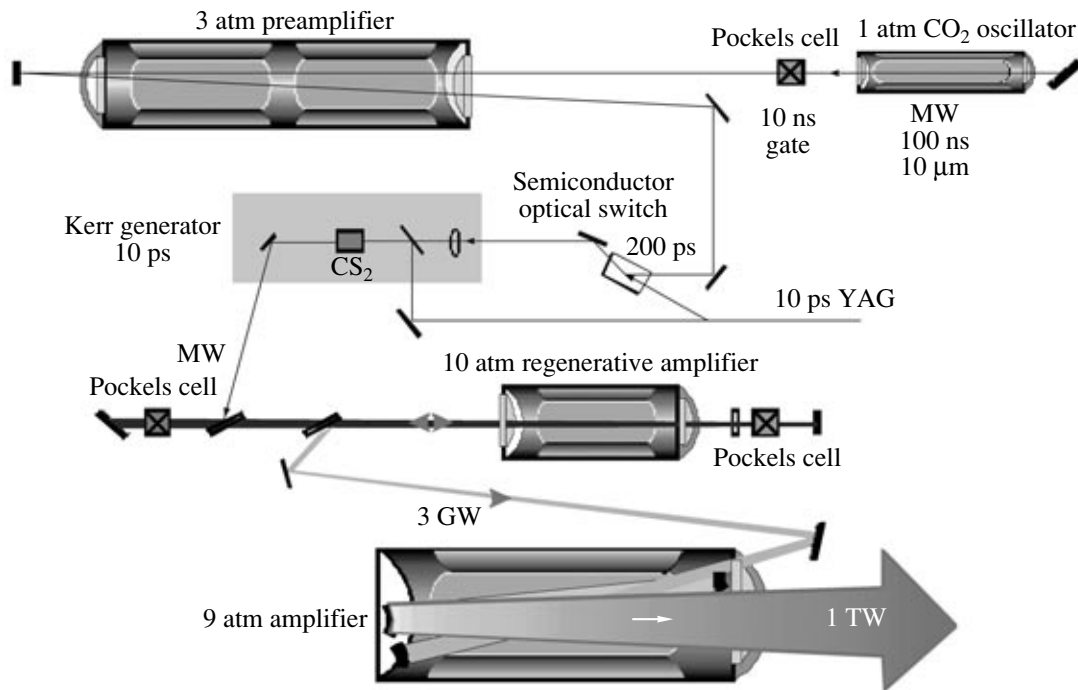


Fig. 1. Optical diagram of a terawatt picosecond CO<sub>2</sub> laser.

laser drivers. The first staged laser acceleration STELLA [1] used this feature to advantage. A controlled energy gain for a large percentage of electrons in a bunch has been achieved since the electron bunch length, as well as mechanical and thermal jitters in the setup, is much less than the laser's 10- $\mu\text{m}$  wavelength.

Let us take into account one more consideration. The degree to which physics is relativistic is determined by a ponderomotive potential. At a given intensity, a 10- $\mu\text{m}$  CO<sub>2</sub> laser reaches a ponderomotive potential 100 times higher than do the 1- $\mu\text{m}$  solid state lasers:

$$W_{\text{osc}} = e^2 E_L^2 / 2m\omega^2, \quad (1)$$

where  $e$  and  $m$  are correspondingly the electron charge and mass and  $\omega$  is the laser frequency  $\omega = 2\pi c/\lambda$ ;  $\lambda$  is the laser wavelength.

This implies the possibility of attaining a proportional increase in the throughput of such processes as electron acceleration and X-ray generation. This feature, again, was demonstrated at the ATF, where the brightest ever Thomson X-ray source was achieved [2] and recently extended into a nonlinear regime [3].

Nevertheless, CO<sub>2</sub> lasers are underutilized for advanced accelerator research due to inherent technical problems. The main difficulty with building ultrafast CO<sub>2</sub> lasers is that their gain spectrum is modulated with a molecular rotational structure that impedes the amplification of short picosecond pulses. Fortunately, this bandwidth limitation can be alleviated by pressure broadening at or above 10 atm of laser gas pressure or

by using multiisotope gas mixtures [4]. The ATF's CO<sub>2</sub> laser system incorporates such high-pressure-gas laser technology.

The principal elements in the ATF laser start with a conventional 1-atm pulsed 100-ns CO<sub>2</sub> oscillator (see Fig. 1). A mode-locked 10-ps Nd : YAG laser selects 10- $\mu\text{m}$  pulses of equivalent duration by rotating their polarization in a Kerr cell. To improve contrast and increase the intensity of a seed pulse going into an amplifier, we use several intermediate pulse-chopping techniques. First, a 10-ns pulse is cut from the oscillator's output with a Pockels cell, and this signal is amplified in a preamplifier that does not need to be of critically high pressure. Next, we use a split portion of the YAG beam on a semiconductor optical switch to select a 200-ps pulse due to the 10- $\mu\text{m}$  reflection from naturally decaying free carriers produced by the 1- $\mu\text{m}$  irradiation. Only after this is the 10 ps CO<sub>2</sub> laser pulse cut in a Kerr switch.

A 10-atm regenerative amplifier traps the seed pulse for several double passes and releases it when the power reaches a several GW level. Finally, another high-pressure amplifier with a bigger aperture boosts the energy to 10 J and the peak power close to the 1 TW level. The ATF plans upgrades to 3 ps pulses and later to 1 ps pulses to attain multiterawatt laser power.

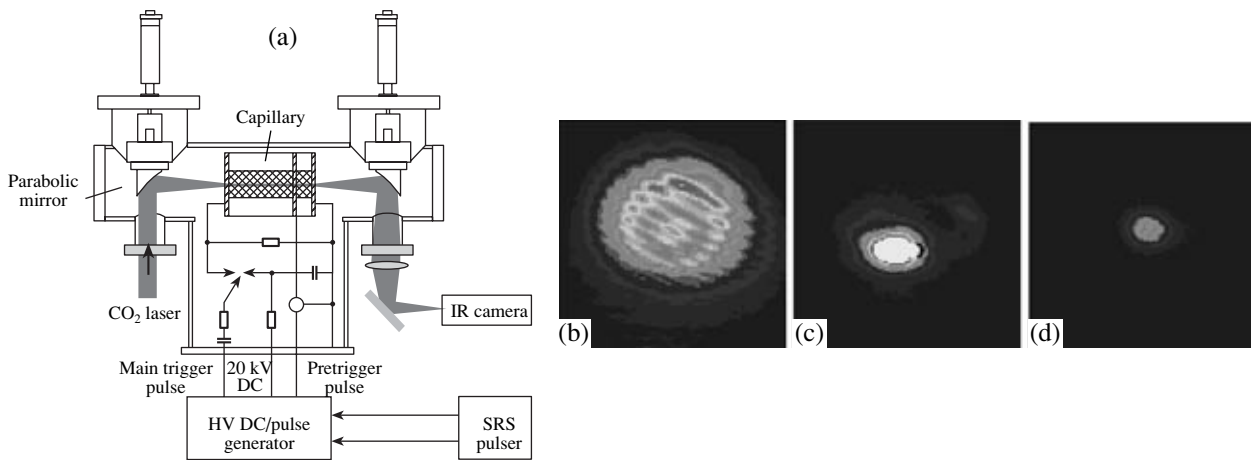


**Fig. 2.** Channeling of a high-power CO<sub>2</sub> laser in a capillary discharge plasma: (a) principle diagram; (b) laser beam image 18 mm behind the focal point, free space propagation; (c) compressed laser beam after the 18-mm-long capillary discharge, no attenuation adjustment to compare with (b); (d) same as (c) but with an attenuation increased to show an unsaturated image with  $w_0 = 160 \mu\text{m}$  FWHM.

### CAPILLARY DISCHARGE: A PLASMA SOURCE

A plasma source was developed for guiding a CO<sub>2</sub> laser in the LWFA and similar experiments that require a long laser focus. Using plasma as an optical guide necessitated building a radial electron-density distribution with the minimum at the axis. Then, the refraction index profile resembles one observed in a gradient index optical fiber. The laser beam is trapped along the axis of such a plasma fiber due to the total internal reflection. One way to produce such a plasma profile is by providing an actively triggered vacuum discharge inside a polypropylene capillary tube. The hydrogen-carbon plasma is generated by the ablation of a plastic wall. Simulations show that electron density distribution is controlled primarily by the Joule heating and is suitably profiled for guiding CO<sub>2</sub> laser beams. This scheme was first developed and tested at Hebrew University, Jerusalem [5], and refined at the ATF, where we added the necessary sophistication to accurately align a capillary along the electron and laser beams.

We reported CO<sub>2</sub> laser channeling in a capillary discharge [6]. A laser beam was focused at the capillary's entrance with a parabolic mirror (Fig. 2a). The laser beam is picked up from the capillary's exit for imaging on an IR video camera.

Figures 2b–2d show the resulting images. The first one, Fig. 2b, illustrates how the laser beam diverges from the focus over the 18-mm distance in a free space. Then, after the 18-mm-long 30-kV capillary discharge, we observe a guided beam of 160 μm FWHM (Figs. 2c, 2d) that is much smaller than the capillary's 1-mm physical diameter. This was the first experimental demonstration of guiding the 10-μm laser beam in a plasma channel.

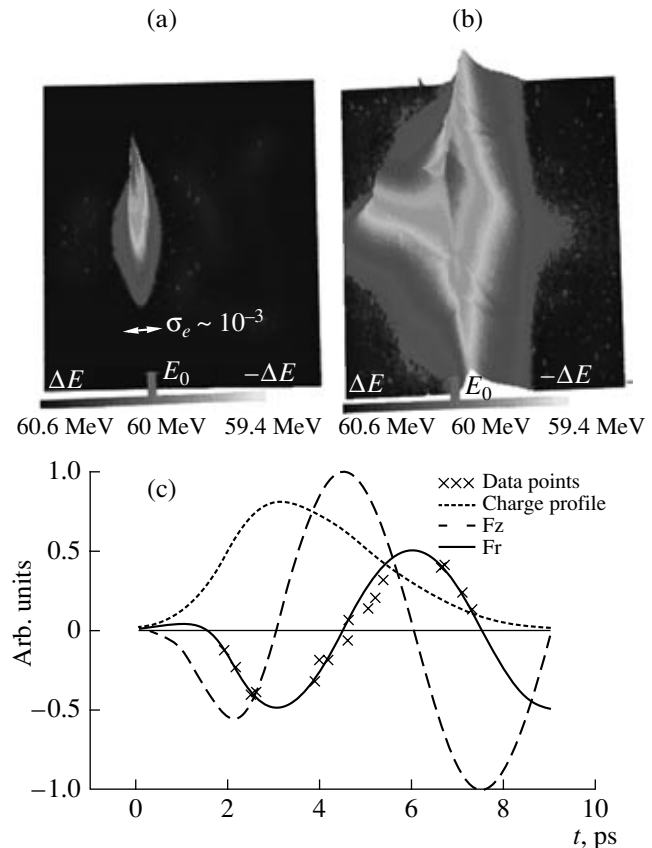


**Fig. 3.** Electron density distributions on a spectrometer reveal the 90° phase shift between the longitudinal and transverse components in the plasma wake. Horizontal and vertical directions on the spectrometer screen correspond to the energy spread and angular spread of the *e* beam: (a) *e*-beam distribution obtained without plasma; (b) *e* beam after passing plasma; (c) theoretical and experimental temporal plots: dotted line—*e*-beam pulse (experimental), dashed line—longitudinal wake field (theoretical), solid line—transverse wake field (theoretical), crosses—experimental points.

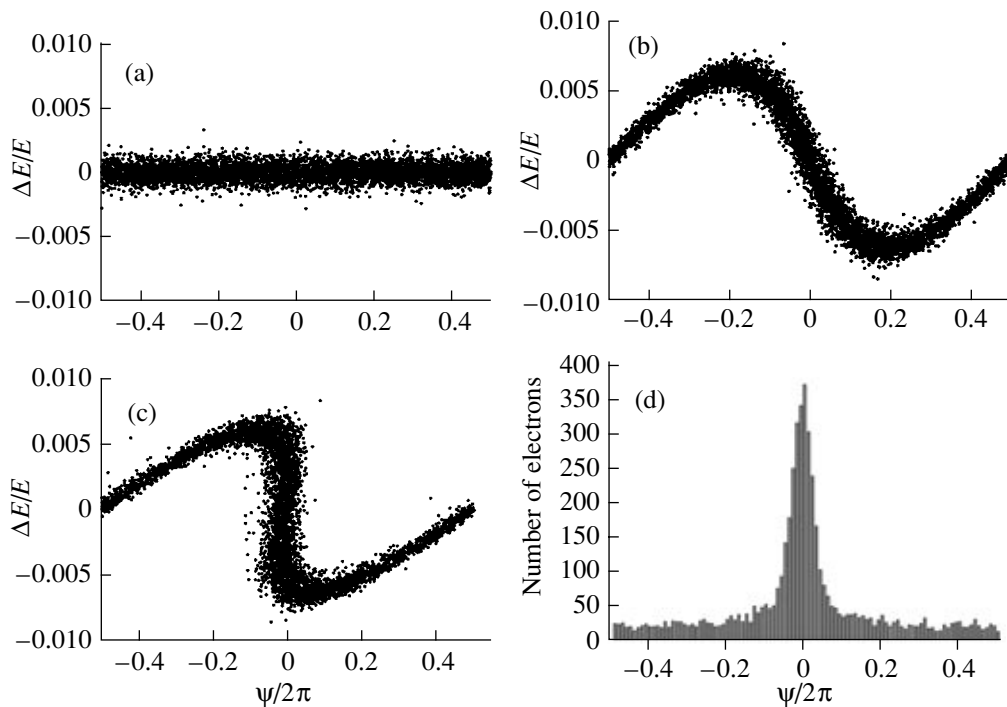


**Fig. 4.** Simulations of the  $e$ -beam bunching: (a) initial uniform energy distribution; (b) energy modulation at the wiggler exit; (c) energy distribution at the entrance to the second wiggler; (d) longitudinal density distribution at the entrance to the second wiggler.

## PLASMA WAKEFIELD STUDY

Next, we transmitted a relativistic  $e$  beam through a plasma channel to observe and study plasma wakefields.

Figures 3a and 3b show the electron distributions recorded with an electron spectrometer placed after the capillary. The horizontal axis shows electron energy span, and the vertical axis represents transverse  $e$ -beam size that is proportional to an angular divergence in the  $e$  beam. Figure 3a was obtained with the plasma off and shows the  $e$  beam's natural energy spread and transverse dimensions. Figure 3b was obtained with the plasma on and shows that parts of the beam loose energy, while other parts gain energy. At the same time, the  $e$  beam is focused or defocused in a peculiar pattern that is correlated with the energy gain. This pattern is explained in reference [7]. The leading edge of the electron bunch excites a plasma wake. It was predicted, but never experimentally proved, that the transverse force in the plasma wake has a  $90^\circ$  offset from the longitudinal force, as is shown in Fig. 3c. Then, depending upon the wakefield phase, electrons with the same longitudinal momentum can form two groups: focused and defocused. This explains why the best fit to corresponding vertical slices from the spectral distribution in Fig. 3b is a superposition of two Gaussian distributions. From the width of the individual Gaussian distribution for each group of electrons, we reconstructed the transverse force and obtained a perfect fit to the theoretical depen-

dence (crosses on Fig. 3c). This finding confirms the prediction of a phase offset between the accelerating and focusing components of a plasma wake.

These first ATF experiments on manipulating laser and relativistic electron beams through a capillary discharge, which is integrated into the linac's beamline, opened an opportunity to launch an experimental program on advanced methods of electron acceleration in plasma. A "microbunch factory," described in the next paragraph, added further distinction to the ATF's research program.

## ELECTRON MICROBUNCHING TECHNOLOGY

A periodic permanent magnet array placed into the linac's beamline causes electrons to oscillate or wiggle. A linearly polarized laser beam, co-propagating with the electrons, gives an additional kick to them at each turn of their trajectory when the phase-matching condition is satisfied:

$$\gamma^2 = \frac{\lambda_w}{2\lambda} \left( 1 + \frac{K_w^2}{2} \right), \quad (2)$$

where  $\lambda_w$  is the wiggler period,  $\gamma$  is the Lorentz factor,  $K_w$  is the wiggler strength parameter  $K_w = eB_0\lambda_w/2\pi mc$ , and  $B_0$  is the peak magnetic field. The outcome of such energy modulation imposed on the  $e$  beam by a laser inside the wiggler is microbunching.

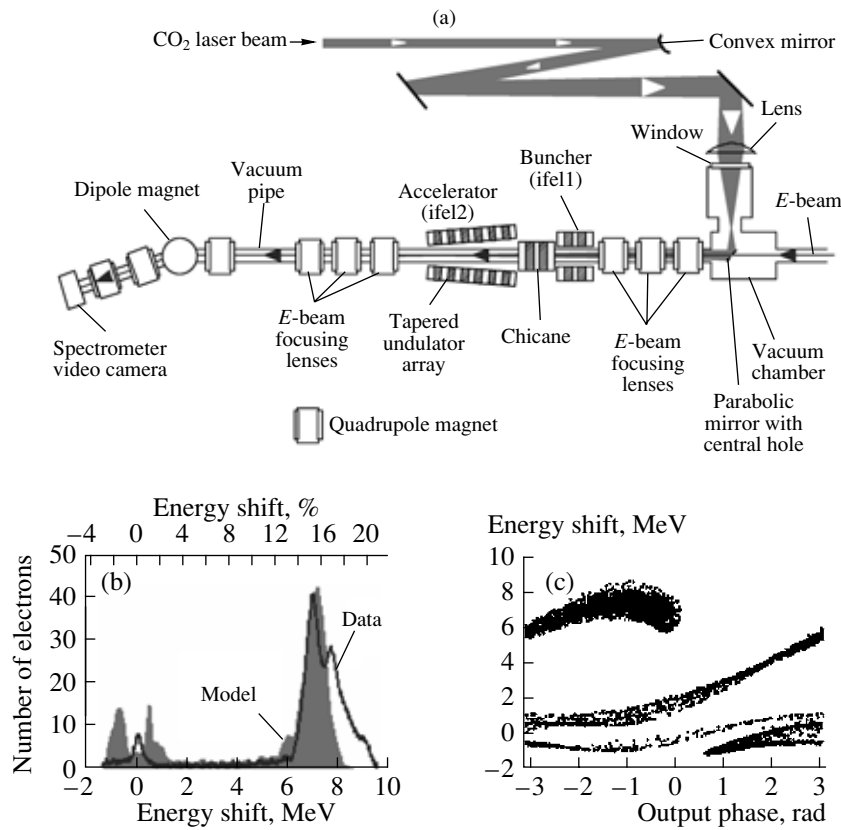


**Fig. 5.** STELLA II experiment: (a) diagram of a setup; (b) comparison of experimental spectra observed after the 2nd wiggler (line) with simulations (histogram); (c) simulated electron phase space.

The process of microbunching is illustrated by modeling on Fig. 4, which assumes practically achievable parameters for the  $e$ -beam and  $\text{CO}_2$  laser. If the  $e$ -beam energy is sinusoidally modulated by the laser inside a wiggler and electrons are allowed to drift, they group together into 3-fs-long microbunches, exactly periodical to the laser wavelength. Such bunches, which are ten times shorter than the  $\text{CO}_2$  laser wavelength, can be used for monoenergetic laser acceleration, as was demonstrated at the ATF in the first staged laser electron acceleration experiment (abbreviated to STELLA), wherein two wigglers were placed in-line and injected with electron and  $\text{CO}_2$  laser beams.

In the initial STELLA experiment, the  $\text{CO}_2$  laser beam was split between two wigglers; the first one introduced bunching, while the second directed acceleration of the microbunches [1].

In the second version of the same experiment, STELLA II, a more compact configuration was used (Fig. 5a), with a single 30-GW laser beam penetrating both wigglers; this afforded better phase control between stages and used the laser energy more efficiently. Microbunched electrons trapped in the laser field produce a sharp peak in a spectrum (Fig. 5b). The experimental result matched simulations [8]. A more spectacular result could be expected with the terawatt

$\text{CO}_2$  power now available. However, the ATF users, utilizing the unique capabilities of the microbunched  $e$  beam in a different way, have turned their attention to plasma acceleration, as discussed next.

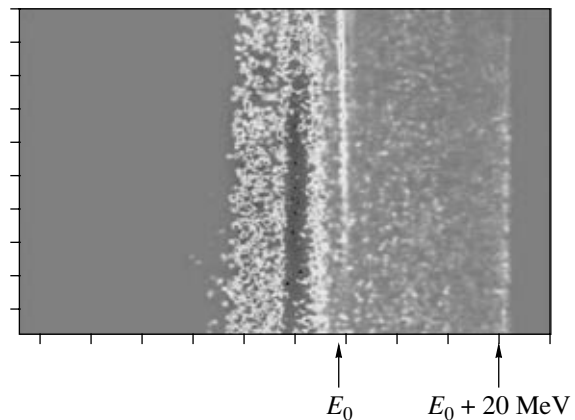


**Fig. 6.** Simulated witness spectrum for the resonant PWFA after passing 3-mm-thick plasma. Arrow labeled  $E_0$  corresponds to the initial  $e$ -beam energy.

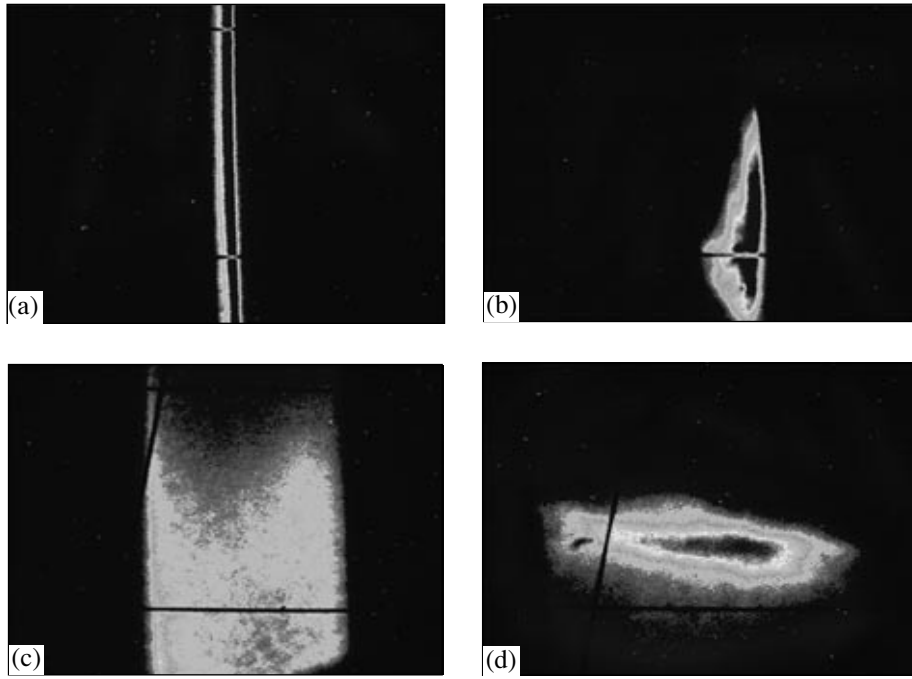


**Fig. 7.** Focusing of a bunched  $e$  beam in a plasma: (a) no plasma, no laser; (b) plasma, no laser; (c) no plasma, laser; (d) plasma and laser.

### RESONANT WAKEFIELD EXCITATION

A new spin-off from the ATF's microbunching technique is a novel idea on resonant wakefield excitation. This study builds on the recent success of the ATF's work on wakefields and those for STELLA, where the ATF provides the necessary components to investigate a PWFA scheme wherein a train of bunches is fed into a high-density ( $n_e = 10^{19} \text{ cm}^{-3}$ ) plasma. Another predecessor to this project is the E162 experiment at SLAC, which demonstrated the acceleration of both positrons and electrons in meter-scale plasmas driven by the 30-GeV linac [9]. That experiment is related to the afterburner concept, which uses two separated bunches as the driving and accelerated beams. It is now believed that realization of the promise of plasma wakefield accelerators will require employing multiple bunches.

When the periodical bunch train enters a plasma that has a resonance wavelength

$$\lambda_p (\mu\text{m}) = \frac{c}{e} \left( \frac{\pi m}{n_e} \right)^{1/2} \approx \frac{3.3 \times 10^{10}}{\sqrt{n_e (\text{cm}^{-3})}} \quad (3)$$

equal to the separation distance of the bunches, a strong wakefield will be driven to an amplitude that is at least one order of magnitude higher than that of a non-bunched beam.

The simulations in Fig. 6 depict the modulation of the electron bunches' energy, starting from the initial narrow energy spectrum, after 3-mm propagation through the plasma. As electrons primarily lose their

energy, it goes into exciting a plasma wake. The amount of the deceleration increases as the wake's amplitude grows. We note that the particles that are accelerated are background residual electrons spread between microbunches, where they serve as probes of the wakefields. The maximum acceleration reaches 20 MeV, which is equal to the 60-MeV/cm peak field multiplied by the plasma's length.

In the first run of the ATF's PWFA experiment, the resonance condition was not reached. Meanwhile, we observed an unexpected effect due to the strong focusing of the bunched electron beam (Fig. 7). The beam's vertical compression increases with the stronger electron-energy modulation caused by the laser beam in a wiggler. The expression for the focusing strength in a plasma wave

$$K = \frac{eE_0 k_p}{\gamma m c^2 (k_p \sigma_r)^2}, \quad (4)$$

where  $E_0$  is the wakefield amplitude and  $\sigma_r$  is the initial  $e$ -beam rms radius, implies that this additional focusing effect is due to the amplitude of a plasma wakefield that is proportional to the extent of modulation of the electron energy. This tentative conclusion awaits confirmation.

### SEEDED LWFA

Finally, we discuss the LWFA experiment initiated at the ATF by the STELLA collaboration. The

STELLA-LWFA experiment will attempt to make several first observations. In fact, this will be the first demonstration of the LWFA process using a CO<sub>2</sub> laser beam as a driver of the wakefield. The 10- $\mu\text{m}$  wavelength of the CO<sub>2</sub> laser beam is 10 times longer than that of solid state lasers typically used in LWFA research. As mentioned above, one of its advantages is the hundredfold increase in ponderomotive potential, or the tenfold increase in the laser-strength parameter

$$a_0 \equiv eE_L/\omega mc \approx 4.8 \times 10^{-6} \sqrt{P_L} \frac{\lambda}{w_0}, \quad (5)$$

which directly benefits the LWFA process

$$E_{\text{acc}}^{\text{max}} [\text{GV/m}] = \frac{mc^2 2\pi}{e \lambda_p} \frac{a_0^2/2}{(1 + a_0^2/2)^{1/2}} \quad (6)$$

$$\approx 2.8 \times 10^4 (\lambda/w_0)^2 P_L [\text{TW}]/\lambda_p [\mu\text{m}],$$

where  $P_L$  and  $w_0$  are, correspondingly, the laser power and the focal spot's radius.

This will probably be the first attempt to perform the LWFA in a plasma channel—an approach considered very advantageous for developing the next-generation LWFA.

In a standard resonant LWFA, the laser pulse's length typically is very short in order to resonantly excite a plasma wave

$$\tau_L \approx \lambda_p/2c. \quad (7)$$

The self-modulated regime (SM-LWFA) differs from the resonant LWFA in that the laser pulse's length is intentionally relatively long but very intense, with

$$P_L (\text{GW}) \geq P_{\text{cr}} \approx 17.4 (\lambda_p/\lambda)^2. \quad (8)$$

That characteristic allows for relativistic self-focusing and Raman instabilities that modulate the laser pulse in the resonance with the plasma wake. This, in turn, enhances the wake's amplitude to the wavebreaking:

$$E_{\text{wb}}^{\text{max}} = \frac{mc^2 2\pi}{e \lambda_p} \sqrt{\frac{2\lambda_p}{\lambda}}. \quad (9)$$

The laser pulse used in the STELLA-LWFA experiment is considerably longer than  $\lambda_p/2c$ , and the laser power is below  $P_{\text{cr}}$ . To improve the efficiency of producing the wake, an  $e$ -beam pulse will act as a seed to generate a wakefield that will then be enhanced by the laser pulse in the fashion used in the SM-LWFA experiment. This mechanism, called seeded self-modulated LWFA [10], affords better control over electron acceleration, since it runs in a linear regime well below wavebreaking. Another bunch with a variable delay will be sent to probe the wakefield; this, too, is a new feature in LWFA experiments.

Figure 8 shows the model's predictions for the seeded LWFA process. The seed  $e$ -beam pulse initiates

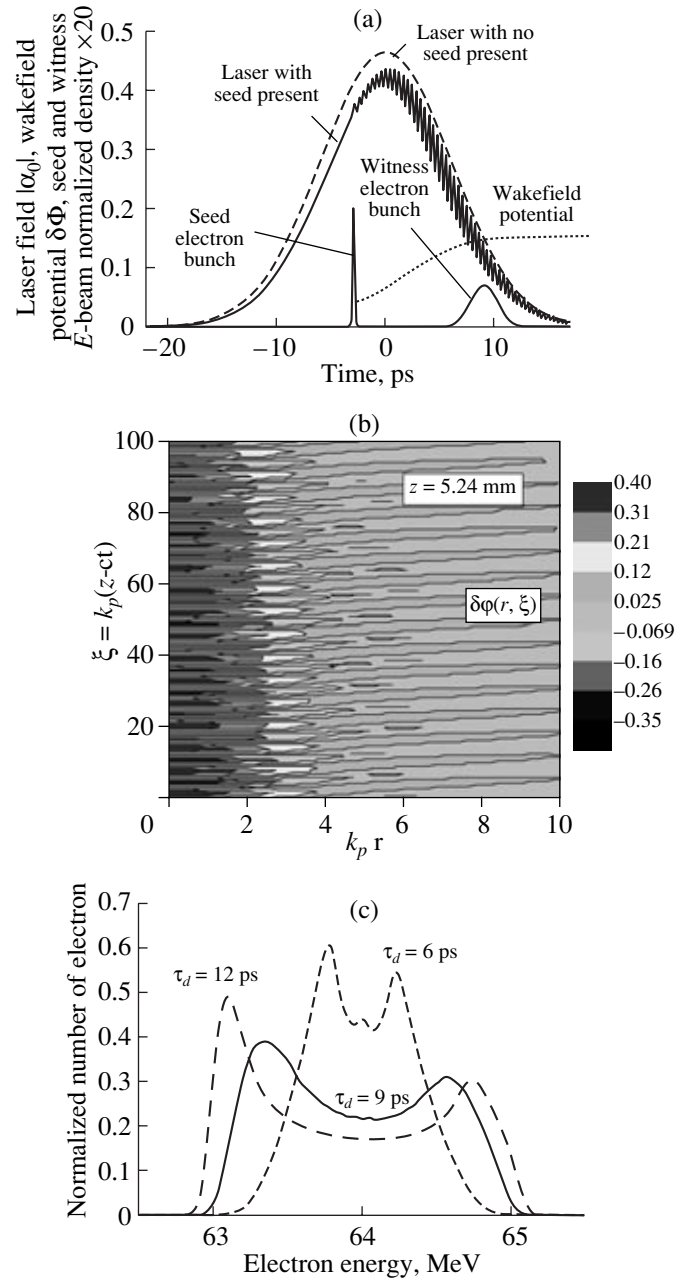


**Fig. 8.** Model predictions for a seeded LWFA experiment: (a) laser and wakefield strength; modulation is imposed on the laser pulse by the wakefield initiated by a seed electron bunch; (b) wakefield potential versus longitudinal and transverse coordinates; (c) electron energy spectrum of witness  $e$ -beam pulse for a plasma acceleration length of 2 mm as a function of the time delay between the seed and witness  $e$ -beam pulses.

the formation of a longitudinal wakefield, whose amplitude is increased by the laser pulse (see Fig. 8a). This wakefield interacts with the laser field, thereby modulating the laser beam's envelope. The model simulations show that performance is better when the wakes produced by the seed  $e$ -beam pulse encounter the high laser fields present near the peak of the laser pulse.

Therefore, the laser pulse will actually arrive slightly before the seed  $e$ -beam pulse. A second “witness”  $e$ -beam pulse will probe the wakes that reach the maximum amplitude near the tail end of the laser pulse. The witness electrons experience energy modulation caused by the wakefield, which can be measured by an energy spectrometer.

Simulations show that, to generate a strong longitudinal wakefield with the available 10-ps CO<sub>2</sub> laser, the plasma density must be  $n_e \sim 1 \times 10^{17} \text{ cm}^{-3}$  and the seed  $e$ -beam pulse length must be very short ( $< 200 \text{ fs}$ ). Sending the ATF  $e$  beam through a chicane, which compresses the  $e$  beam’s pulse length, will generate this femtosecond  $e$ -beam pulse. Generating the second  $e$ -beam pulse was demonstrated at the ATF by splitting the UV-laser pulse into two pulses and sending them into the linac’s photocathode gun in series.

The simulated wakefields are fairly regular (Fig. 8b), indicative of a linear wakefield regime. Indeed, for the STELLA-LWFA experimental parameters,  $a_0 \approx 0.5$ , whereas the wavebreaking laser strength obtained from Eqs. (6) and (9) is  $a_0^{wb} \approx 2\sqrt{\lambda_p/\lambda} \approx 4\text{--}5$ .

The strongest wakefields extend to a radial distance of  $\sim 50 \mu\text{m}$ . Thus, we plan to focus witness bunches within  $\sigma_r \approx 20 \mu\text{m}$ .

Figure 8c plots the simulated energy spectrum of the witness bunch separated by different time intervals after the seed. There is a classic double-peak energy spectrum for an acceleration length  $L_{\text{acc}} = 2 \text{ mm}$  corresponding to sinusoidal modulation of the  $e$ -beam energy similar to one observed with an IFEL buncher. The peak modulation appears to reach a steady-state value for separations greater than  $\sim 10 \text{ ps}$ . For  $L_{\text{acc}} = 3 \text{ mm}$ , modulation is higher, but it becomes asymmetric as the dephasing length is passed:

$$L_{\text{ph}} = \lambda_p^3/\lambda^2. \quad (11)$$

Note that the LWFA modulator can be suitable for making microbunches. These microbunches can be subsequently trapped and accelerated in a second LWFA acceleration stage. This second LWFA stage will be

investigated in future phases of the STELLA-LWFA experiment.

## CONCLUSIONS

The high-brightness 70-MeV linac, picosecond TW CO<sub>2</sub> laser, plasma channel, and microbunching technique all available at Brookhaven’s ATF will allow researchers there to initiate a one-of-a-kind program on advanced plasma accelerators. Our preliminary experiments resulted in such milestone achievements as the first staged IFEL accelerator (STELLA), the demonstration of phasing between the wakefield components, and the channeling of a high-power CO<sub>2</sub> laser beam in a plasma. Next-generation experiments on seeded and probed LWFA and resonant multibunch PWFA are already in progress.

## ACKNOWLEDGMENTS

This work is supported by the US Department of Energy.

## REFERENCES

1. W. D. Kimura, *et al.*, Phys. Rev. Lett. **86**, 4041 (2001).
2. I. V. Pogorelsky, *et al.*, Phys. Rev. **3**, 090 702 (2000).
3. M. Babzien, *et al.*, Phys. Rev. Lett. (2005) (in press).
4. I. V. Pogorelsky, *et al.*, IEEE J. Quantum Electron. **31**, 556 (1995).
5. D. Kaganovich, *et al.*, Appl. Phys. Lett. **71**, 2925 (1997).
6. I. V. Pogorelsky, *et al.*, Appl. Phys. Lett. **83**, 3459 (2003).
7. V. Yakimenko, *et al.*, Phys. Rev. Lett. **91**, 014 802 (2003).
8. W. D. Kimura, *et al.*, Phys. Rev. Lett. **92**, 054 801 (2004).
9. B. Blue, *et al.*, Phys. Rev. Lett. **90**, 214 801 (2003); C. Joshi, in *Proceedings of 11th Advanced Accelerator Concepts Workshop, Stony Brook, New York, USA, 2004* (New York, 2004), p. 3.
10. L. C. Steinhauer, W. D. Kimura, and R. N. Agarwal, in *Proceedings of International Conference on Lasers, Tucson, 2001* (STS, Tucson, 2001), p. 159.